

## Comparison of the Biophysical Properties of Racemic and *d-Erythro-N*-Acyl Sphingomyelins

Bodil Ramstedt and J. Peter Slotte

Department of Biochemistry and Pharmacy, Åbo Akademi University, FIN 20521 Turku, Finland

**ABSTRACT** In this study stereochemically pure *d-erythro*-sphingomyelins (SMs) with either 16:0 or 18:1<sup>cisΔ9</sup> as the *N*-linked acyl-chain were synthesized. Our purpose was to examine the properties of these sphingomyelins and acyl-chain matched racemic (*d-erythro/l-threo*) sphingomyelins in model membranes. Liquid-expanded *d-erythro-N*-16:0-SM in monolayers was observed to pack more densely than the corresponding racemic sphingomyelin. Cholesterol desorption to  $\beta$ -cyclodextrin was significantly slower from *d-erythro-N*-16:0-SM monolayers than from racemic *N*-16:0-SM monolayers. Significantly more condensed domains were seen in cholesterol/*d-erythro-N*-16:0-SM monolayers than in the corresponding racemic mixed monolayers, when [7-nitrobenz-2-oxa-1,3-diazol-4-yl]phosphatidylcholine was used as a probe in monolayer fluorescence microscopy. With monolayers of *N*-18:1-SMs, both the lateral packing densities (sphingomyelin monolayers) and the rates of cholesterol desorption (mixed cholesterol/sphingomyelin monolayers) was found to be similar for *d-erythro* and racemic sphingomyelins. The phase transition temperature and enthalpy of *d-erythro-N*-16:0-SM in bilayer membranes were slightly higher compared with the corresponding racemic sphingomyelin (41.1°C and  $8.4 \pm 0.4$  kJ/mol, and 39.9°C and  $7.2 \pm 0.2$  kJ/mol, respectively). Finally, *d-erythro*-sphingomyelins in monolayers (both *N*-16:0 and *N*-18:1 species) were not as easily degraded at 37°C by sphingomyelinase (*Staphylococcus aureus*) as the corresponding racemic sphingomyelins. We conclude that racemic sphingomyelins differ significantly in their biophysical properties from the physiologically relevant *d-erythro* sphingomyelins.

### INTRODUCTION

Sphingomyelins are important components of the external leaflet of cellular plasma membranes. Naturally occurring sphingomyelins consist of long-chain sphingosine or sphinganine bases, and long and highly saturated amide-linked acyl chains. The gel-to-fluid (or order-to-disorder) transition temperatures of natural sphingomyelins are fairly high (30–45°C) compared with other naturally occurring phospholipids (Barenholz and Thompson, 1980). These features give natural sphingomyelins and glycosphingolipids the potential to introduce lateral heterogeneity in the membrane plane (Bar et al., 1997; Barenholz and Thompson, 1980). Studies with various cell membranes have suggested that sphingomyelins and glycosphingolipids may cluster with cholesterol in biological membranes to form raft-like domains (reviewed in Simons and Ikonen, 1997; Brown, 1998; Brown and Rose, 1992; Harder and Simons, 1997).

Sphingomyelin is highly enriched in the plasma membrane compartment, as is cholesterol (Lange et al., 1989; Lange and Ramos, 1983). It is also likely that sphingomyelin and cholesterol colocalize in the membrane, because cholesterol has been shown to prefer to interact with sphingomyelin in cell membranes (Ohvo et al., 1997; Pörn et al., 1993). The possibility of a specific hydrogen bond between the 3-OH group in cholesterol and sphingomyelin has been

discussed in the literature (Barenholz and Thompson, 1980; Boggs, 1987). The hydroxyl group at C-3 in sphingomyelin has been shown not to affect the interaction with cholesterol in model membranes (Grönberg et al., 1991; Kan et al., 1991). The amide group at C-2 in sphingomyelin, on the other hand, has been shown to be essential for the strong interaction with cholesterol, because replacement of this group increases the availability of cholesterol in mixed vesicles for oxidation with cholesterol oxidase (Bittman et al., 1994). The amide-linked acyl chain, its length, its degree of unsaturation, and the position of the possible double bond also influence the interaction with cholesterol (Ramstedt and Slotte, 1999).

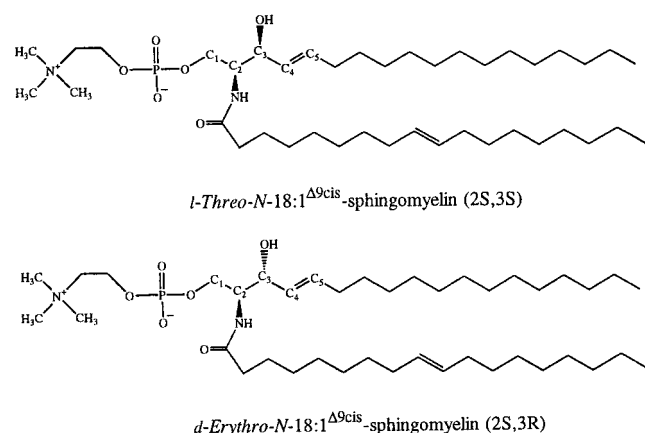
All naturally occurring sphingomyelins have the *d-erythro*-(2S, 3R) configuration of the sphingosine base. However, the synthetic acyl chain-defined sphingomyelins that have been used in most studies on the properties of sphingomyelins in model membranes have been racemic, i.e., they have contained both *d-erythro* and *l-threo* isomers (Sripada et al., 1987; Maulik and Shipley, 1996; Maulik et al., 1991; Bruzik, 1987) (for structural formulas see Scheme 1). This is due to the fact that hydrolysis of sphingomyelin to yield lyso-sphingomyelin (the commonly used synthetic precursor in sphingomyelin synthesis) can give rise to an epimerization at C-3 (Gaver and Sweeley, 1965; Sripada et al., 1987). Most of the commercially available synthetic sphingomyelins have therefore also been racemic. Recently, fully synthetic *d-erythro*-sphingolipids have become available on the market. Consequently, pure *d-erythro*-sphingomyelins have been used in some studies instead of racemic sphingomyelins (Bar et al., 1997). The stereochemistry of sphingolipids has recently been shown to be of biological

Received for publication 5 February 1999 and in final form 31 May 1999.

Address reprint requests to Bodil Ramstedt, Department of Biochemistry and Pharmacy, Åbo Akademi University, P.O. Box 66, FIN 20521 Turku, Finland. Tel.: 358-2-215-4816; Fax: 358-2-215-4745; E-mail: bodil.ramstedt@abo.fi.

© 1999 by the Biophysical Society

0006-3495/99/09/1498/09 \$2.00



Scheme 1

importance, because the fusion of Semliki Forest virus with membranes is dependent on the presence of *d-erythro* sphingolipids in the target membrane in a stereospecific manner (Moesby et al., 1995). In this study, we have synthesized two pure *d-erythro*-sphingomyelins, one saturated (*N*-16:0-SM) and one unsaturated (*N*-18:1<sup>cisΔ9</sup>-SM). The biophysical properties of these sphingomyelins in vesicles and monolayers were then studied, with and without cholesterol, and they were compared to commercial racemic sphingomyelins with the corresponding *N*-linked acyl chains. The racemic sphingomyelins were assumed to contain *d-erythro* and *l-threo* isomers according to previous findings (Sripada et al., 1987; Maulik et al., 1991; Bruzik, 1987).

## EXPERIMENTAL PROCEDURES

### Materials

All lipids (unless otherwise stated) were obtained from Sigma Chemicals (St. Louis, MO), and the sphingomyelins were purified by reverse-phase high-performance liquid chromatography (HPLC) on a LiChrospher 100 RP-18 column (5-μm particle size, 125 × 4 mm column dimensions; Merck, Darmstadt, Germany) before use. Sphingomyelinase (*Staphylococcus aureus*), β-cyclodextrin (CyD), and cyclohexylamine were also obtained from Sigma. Dicyclohexylcarbodiimide (DCC) was obtained from Fluka (Buchs, Switzerland). *d*-Erythro-sphingosylphosphorylcholine (*d*-erythro-SPC) and *l*-threo-sphingosine were obtained from Matreya (Pleasant Gap, PA). Fatty acids were purchased from Larodan AB (Malmö, Sweden). 1,6-Diphenyl-1,3,5-hexatriene (DPH), 1-(4-trimethylammonium-phenyl)-6-phenyl-1,3,5-hexatriene (TMA-DPH), and [7-nitrobenz-2-oxa-1,3-diazol-4-yl]phosphatidylcholine (NBD-PC) were obtained from Molecular Probes (Leiden, the Netherlands). Stock solutions of lipids were prepared in hexane/2-propanol (3/2, v/v), stored in the dark at -20°C, and warmed to ambient temperature before use. The cyclodextrin stock solutions were prepared in pure water to a concentration of 40 mM. The water used as the subphase for the monolayers and for differential scanning calorimetry (DSC) measurements was purified by reverse osmosis followed by passage through a Millipore UF Plus water purification system, to yield a product with a resistivity of 18.2 MΩ-cm. The solvents used for synthesis of phospholipids were stored over Molecular Sieves 4A (Merck).

### Synthesis of *d-erythro*-sphingomyelins

Pure *d-erythro*-sphingomyelins were synthesized from *d-erythro*-SPC and free fatty acids as described previously (Cohen et al., 1984; Ramstedt and

Slotte, 1999). The sphingomyelins formed were initially purified using bonded phase columns according to the method of Kaluzny et al. (1985), followed by reverse-phase HPLC on a LiChrospher 100 RP-18 column (5-μm particle size, 125 × 4 mm column dimensions), using methanol at a flow of 1 ml/min. After these purification steps, the sphingomyelins gave a single spot when analyzed by high-performance thin-layer chromatography (HPTLC), developed with chloroform/methanol/acetic acid/water (25/15/4/2, v/v) (Skiński et al., 1964). The identity of the synthesized *d-erythro* sphingomyelin was positively verified by <sup>1</sup>H-NMR, as described by Bruzik (1988).

### Long-chain base extraction and analysis

To study the base composition of the sphingomyelins, basic hydrolysis with barium hydroxide in warm dioxane was performed to give the sphingosine bases and free fatty acids (Morrison and Hay, 1970). This procedure does not give epimerization at C-3 of the sphingosine base. The sphingosine bases were extracted with hexane. HPLC analysis of *o*-phthalaldehyde-base derivatives was performed on a Spherisorb S 5 ODS2-column (Phase Sep, Queensferry, England). The separation was made with 0.5 ml/min methanol/5 mM phosphate buffer (pH 7.0; 92.5/7.5, v/v) as the mobile phase, and the bases were detected with a Shimadzu RF-530 fluorescence monitor (Kyoto, Japan), with excitation and emission at 340 and 455 nm, respectively, as described by Wilson and co-workers (1988).

### Force-area isotherms

Pure monolayers of each lipid were compressed on water at ambient temperature with a KSV surface barostat (KSV Instruments, Helsinki, Finland). Data were collected using proprietary KSV software. Surface pressure versus mean molecular area information was acquired, and the surface compressional modulus of the sphingomyelin monolayers was subsequently derived from these data as the reciprocal of the isothermal compressibility, as described previously (Smaby et al., 1996).

### Monolayer fluorescence microscopy

The formation of lateral cholesterol-rich domains in mixed cholesterol-sphingomyelin monolayers was determined with monolayer fluorescence microscopy, using NBD-PC as a fluorescent probe (at 1 mol%). Micrographs were obtained using a sensitive video camera attached to a DT3851 digitizing board in a personal computer (Slotte, 1995; Slotte and Mattjus, 1995). The lateral domains were documented at 1 mN/m after a monolayer compression/expansion cycle.

### Removal of monolayer cholesterol to the subphase by cyclodextrins

Mixed monolayers containing phospholipids and 60 mol% cholesterol were prepared at the air/water interface. The trough used was of a zero-order type, with a reaction chamber (23.9 ml volume, 28.3 cm<sup>2</sup> area) separated by a glass bridge from the lipid reservoir (Ohvo and Slotte, 1996; Verger and de Haas, 1973). The cyclodextrin (CyD) (in a volume not exceeding 1 ml) was injected into the reaction chamber, the content of which was continuously stirred (22°C). The final CyD concentration in the subphase was 1.7 mM. The removal of lipids from the monolayer to the subphase was determined from the area decrease of the monolayer at constant surface pressure (20 mN/m), as described by Ohvo and Slotte (1996).

### Differential scanning calorimetry

Sphingomyelins were dissolved in hexane and 2-propanol (3:2 v/v). The solvent was evaporated at 40°C under a stream of argon. Excess solvent

was removed by vacuum drying at room temperature for at least 6 h. The lipids were then suspended in water by warming the tube to 50°C and vortexing vigorously for ~30 s. The water used as reference and the lipid suspensions were degassed under vacuum. The lipid suspension and water were loaded into the sample and reference cell, respectively, of a Nano II high-sensitivity scanning calorimeter (Calorimetric Science Corporation, Provo, UT). Heating scans from 20°C to 60°C at a scan rate of 0.3°C/min were performed. Three consecutive heating scans were made on both samples, giving identical thermograms. Data from two separate preparations of sphingomyelin liposomes were analyzed and averaged.

### Determination of the steady-state fluorescence anisotropy in unilamellar vesicles

Vesicles were prepared from pure sphingomyelins, or from a mixture of 30 mol% cholesterol and 70 mol% sphingomyelins, using a Lipextruder (Lipex Biomembranes, Vancouver, BC) and the extrusion technique described by Hope and co-workers (1985). In brief, 100 nmol of the lipid, or lipid mixture, was dried under argon. The lipids were then sonicated in water to yield multilamellar vesicles (MLVs). MLVs were then extruded at 55°C through 400-nm polycarbonate filters (Costar Corp., Cambridge, MA) to yield the desired vesicles. When DPH was used as a reporter molecule for steady-state anisotropy, it was included in the lipid mixture at 0.8 mol% before extrusion. When TMA-DPH was used (0.8 mol%), it was added to preformed vesicles from an ethanolic stock solution. The final ethanol concentration in the assay solution did not exceed 0.5 vol%. Excitation was carried out at 360 nm, and emission was recorded at 430 nm, at a temperature of 37°C, using a Quantamaster 1 spectrofluorimeter operating in the T-format (Photon Technology International, Surrey, England). The steady-state anisotropy,  $r$ , is defined as

$$r = (I_{\parallel} - GI_{\perp}) / (I_{\parallel} + 2GI_{\perp})$$

where  $I_{\parallel}$  and  $I_{\perp}$  are the fluorescence intensities with the analyzer parallel and perpendicular to the vertical polarizer, respectively (Lakowicz, 1983).  $G$  represents the ratio of the sensitivities of the detection system for vertically and horizontally polarized light (Lakowicz, 1983).

### Sphingomyelin hydrolysis in monolayers

Sphingomyelins were hydrolyzed in monolayers by bacterial sphingomyelinase, essentially as described previously (Jungner et al., 1997). The hydrolysis experiments were carried out at 37°C and at a constant surface pressure of 20 mN/m. The final activity of enzyme in the subphase was 6.7 mU/ml for *N*-18:1-SMs and 67 mU/ml for *N*-16:0-SMs.

## RESULTS

### Characterization of the synthetic sphingomyelins

In this study we have synthesized pure *d-erythro-N*-16:0-SM and *d-erythro-N*-18:1<sup>cisΔ<sup>9</sup></sup>-SM and compared them with acyl-matched commercial racemic sphingomyelins. HPTLC analysis of the sphingomyelins gave a single band for the pure *d-erythro*-sphingomyelins, whereas acyl-chain matched racemic sphingomyelins revealed a double-band pattern (Fig. 1). This double band looks similar to the typical double-band pattern of, e.g., bovine brain sphingomyelin, which is due to the variation in acyl chain lengths (data not shown). The double-band pattern shown in Fig. 1 was caused by the fact that the two stereoisomers have different chromatographic properties on HPTLC; the lower band represents the *d-erythro*-isomer, and the upper band

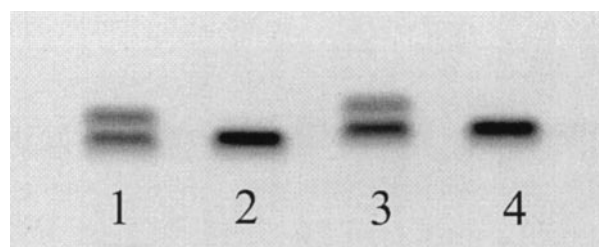


FIGURE 1 Thin-layer chromatographic separation of sphingomyelins. The HPTLC plates were developed with chloroform/methanol/acetic acid/water (25/15/4/2 v/v) and stained with cupric acetate-phosphoric acid reagent. 1, racemic *N*-16:0-SM; 2, *d-erythro*-16:0-SM; 3, racemic *N*-18:1-SM; 4, *d-erythro*-*N*-18:1-SM.

represents the *l-threo*-isomer. To examine the base composition of the sphingomyelins, *o*-phthalaldehyde derivatives of the sphingomyelin bases were analyzed by reverse-phase HPLC (Wilson et al., 1988). As shown in Table 1, the bases of the *d-erythro* SPC and sphingomyelin gave only one peak, corresponding to *d-erythro*-sphingosine. The bases derived from racemic sphingomyelin gave two peaks, one for each stereoisomer of the sphingosine base. No sphinganine could be detected in either racemic or *d-erythro*-sphingomyelins. The *d-erythro* configuration of the synthesized product was further verified by analysis of *d-erythro-N*-18:1-SM by <sup>1</sup>H-NMR. The *d-erythro* configuration could be positively identified, as outlined by Bruzik (1988).

### Interfacial properties of the sphingomyelins

Pure monolayers of the sphingomyelins were prepared at the air/water interface by the surface barostat technique. Fig. 2 shows surface pressure versus mean molecular area isotherms for all sphingomyelins at 22°C (Fig. 2, *A* and *C*) and the surface pressure versus surface compressional modulus (Fig. 2, *B* and *D*). The phase transition region of the *d-erythro-N*-16:0-SM was sharper and occurred at a lower surface pressure than that of the racemic *N*-16:0-SM. The surface compressional modulus of *d-erythro-N*-16:0-SM was markedly lower than the corresponding value measured for racemic *N*-16:0-SM in the transition region (Fig. 2 *B*). *d-Erythro-N*-16:0-SM was also more tightly packed than the

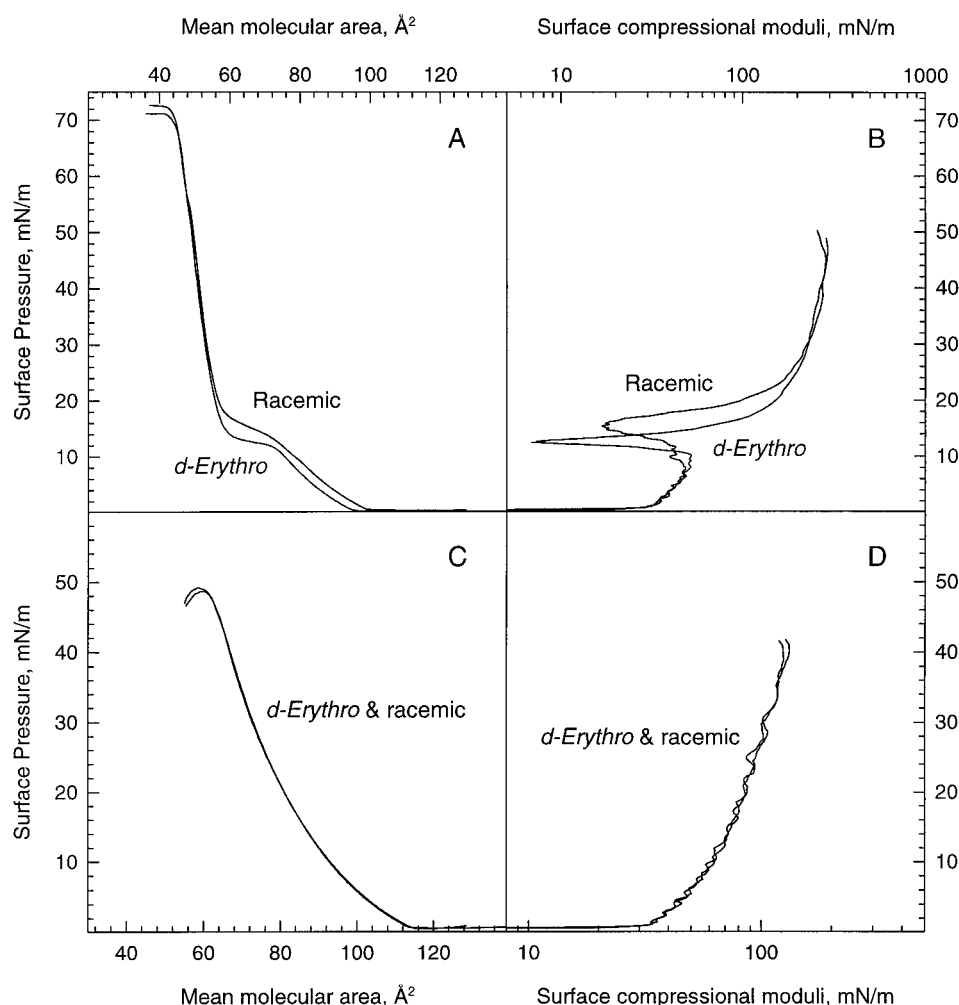
TABLE 1 Sphingomyelin long-chain base analysis with reverse-phase HPLC\*

	<i>l</i> -Threo-sphingosine	<i>d</i> -Erythro-sphingosine	<i>d</i> / <i>l</i> -Erythro-sphinganine
Standards	3.4	3.6	5.1
Racemic <i>N</i> -16:0-SM	3.36	3.52	ND <sup>#</sup>
Racemic <i>N</i> -18:1-SM	3.38	3.55	ND
<i>d-Erythro</i> -SPC	ND	3.60	ND
<i>d-Erythro-N</i> -18:1-SM	ND	3.55	ND

\**o*-Phthalaldehyde derivatives of the bases were analyzed by reverse-phase HPLC on a C18 column. The mobile phase used was methanol/5 mM phosphate buffer (pH 7.0) (92.5/7.5), 0.5 ml/min.

<sup>#</sup>Not detected.

FIGURE 2 Force area isotherms and surface compressional moduli for sphingomyelins. (A) The surface pressure versus mean molecular area isotherms for racemic *N*-16:0-SM and *d-erythro*-*N*-16:0-SM. (C) The surface pressure versus mean molecular area isotherms for racemic *N*-18:1-SM and *d-erythro*-*N*-18:1-SM. (B and D) The surface pressure plotted against the surface compressional moduli for the *N*-16:0-SMs and *N*-18:1-SMs, respectively. The pure monolayers were compressed on water at ambient temperature with a speed not exceeding 10 Å<sup>2</sup>/molecule, min.



racemic *N*-16:0-SM at surface pressures below the transition (i.e., in the liquid-expanded state). For *N*-18:1-SMs the monolayers were liquid-expanded at all surface pressures, and there was no measurable difference in the lateral packing density (Fig. 2 C) or surface compressional modulus (Fig. 2 D) for *d-erythro* or racemic sphingomyelins.

### Lateral phase separation visualized by NBD-phosphatidylcholine partitioning

Monolayers containing *d-erythro* or racemic *N*-16:0-SM with either 20 or 30 mol% cholesterol were prepared at the air/water interface. To study the ability of cholesterol and sphingomyelins to form laterally condensed domains in these monolayers, the partitioning of NBD-PC among the domains was studied, because NBD-PC is known to partition preferentially into loosely packed, liquid-expanded domains, giving these a bright fluorescence (Slotte and Matjusz, 1995; Nag and Keough, 1993). When cholesterol at 20 mol% was mixed with racemic *N*-16:0-SM, a lot of small, dark, cholesterol-rich domains (<1 μm in diameter) were formed in compressed and reexpanded monolayers (Fig. 3 A). In monolayers with 20 mol% cholesterol and *d-erythro*-

*N*-16:0-SM, much larger condensed domains formed (Fig. 3 B), suggesting that cholesterol-rich domains were able to coalesce more easily in *d-erythro*-*N*-16:0-SM monolayers. At 30 mol% cholesterol, large condensed domains were also present in racemic *N*-16:0-SM monolayers (Fig. 3 C). With *d-erythro*-*N*-16:0-SM at 30 mol% cholesterol, the monolayers contained even more and larger condensed domains (Fig. 3 D).

### Cholesterol desorption from mixed monolayers

Cholesterol desorption from monolayers to CyD in the subphase can be used as a measure of how well cholesterol interacts with other lipids in a mixed monolayer (Ohvo and Slotte, 1996). Cholesterol desorption from saturated sphingomyelins is known to be a slow process (Ramstedt and Slotte, 1999). Therefore, we examined cholesterol efflux from monolayers containing a fairly high proportion of cholesterol (i.e., 60 mol%), because the signal-to-noise ratio is increased (Ramstedt and Slotte, 1999). Furthermore, the biological existence of lateral domains with high cholesterol content is most likely, because the lateral distribution of sphingomyelin and cholesterol in biological membranes is



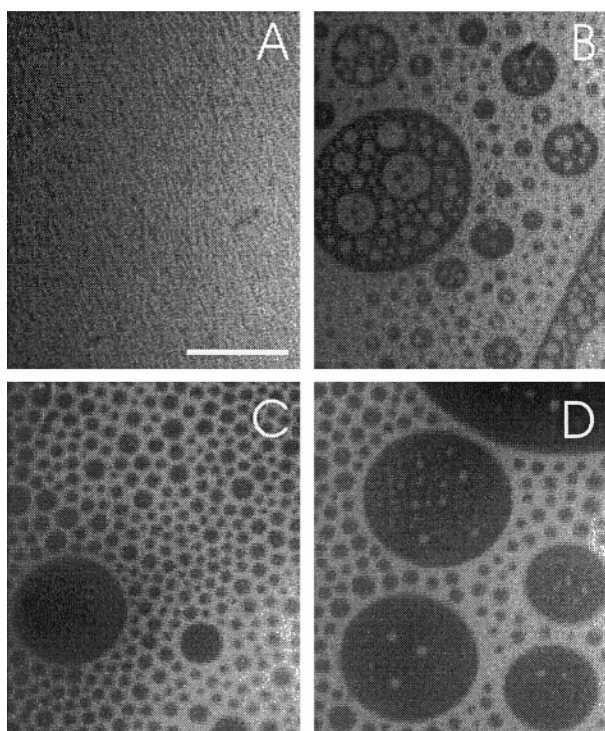


FIGURE 3 Visualization of laterally condensed domains in monolayers of *N*-16:0-sphingomyelin and cholesterol. Monolayers of sphingomyelin were prepared to include 20 mol % (*A* and *B*) or 30 mol % (*C* and *D*) cholesterol together with 1.0 mol % NBD-PC. The monolayers were compressed with a speed not exceeding  $10 \text{ Å}^2/\text{min}$ . The lateral domains were documented at 1 mN/m after a monolayer compression/expansion cycle. Monolayers with racemic *N*-16:0-SM are presented in *A* and *C*, and *B* and *D* show monolayers of pure *d*-erythro-16:0-SM. The scale bar represents  $50 \text{ μm}$ .

very heterogeneous (Schroeder et al., 1996; Brown and Rose, 1992) and because of the apparent colocalization of sphingomyelin and cholesterol in membranes (Lange et al., 1989; Lange and Ramos, 1983; Pörn et al., 1993; Ohvo et al., 1997). As shown in Table 2, the rate of cholesterol desorption was similar for racemic and *d*-erythro-*N*-18:1-SM monolayers, whereas cholesterol desorption from *d*-erythro-*N*-16:0-SM monolayers was significantly lower

**TABLE 2** Cholesterol desorption from mixed monolayers to CyD in the subphase\*

Lipid composition	Desorption rate ( $\text{pmol cm}^{-2} \text{ min}^{-1}$ )
Racemic <i>N</i> -16:0-SM	$5.0 \pm 0.08$
<i>d</i> -Erythro- <i>N</i> -16:0-SM	$3.1 \pm 0.27$
Racemic <i>N</i> -18:1-SM	$15.1 \pm 1.36$
<i>d</i> -Erythro- <i>N</i> -18:1-SM	$16.2 \pm 0.43$

\*Monolayers of sphingomyelin and 60 mol% cholesterol were prepared at the air/water interface. The monolayers were compressed to 20 mN/m and maintained at a constant surface pressure (at ambient temperature). Cholesterol desorption to CyD (1.7 mM) in the subphase was determined as a time function. Values are averages  $\pm$  SD from three separate monolayers of each composition.

than cholesterol desorption from the corresponding racemic *N*-16:0-SM.

### Differential scanning calorimetry

To study the thermodynamics of the gel-to-liquid transition of sphingomyelin bilayers, differential scanning calorimetry was used. Fig. 4 shows representative heating scans of aqueous dispersions of purified racemic *N*-16:0-SM and *d*-erythro-*N*-16:0-SM. The racemic *N*-16:0-SM had a main endothermic transition at  $39.9^\circ\text{C}$ , with a transition enthalpy of  $7.2 \pm 0.2 \text{ kcal/mol}$ . For *d*-erythro-*N*-16:0-SMs both the main transition temperature and the enthalpy were higher ( $41.1^\circ\text{C}$  and  $8.4 \pm 0.4 \text{ kcal/mol}$ , respectively) than that measured for racemic *N*-16:0-SM. The *d*-erythro-*N*-16:0-SM dispersion also showed a small and broad pretransition at  $28.9 \pm 0.1^\circ\text{C}$  ( $\Delta H = 0.5 \pm 0.2 \text{ kcal/mol}$ ), which was not seen for the racemic *N*-16:0-SM.

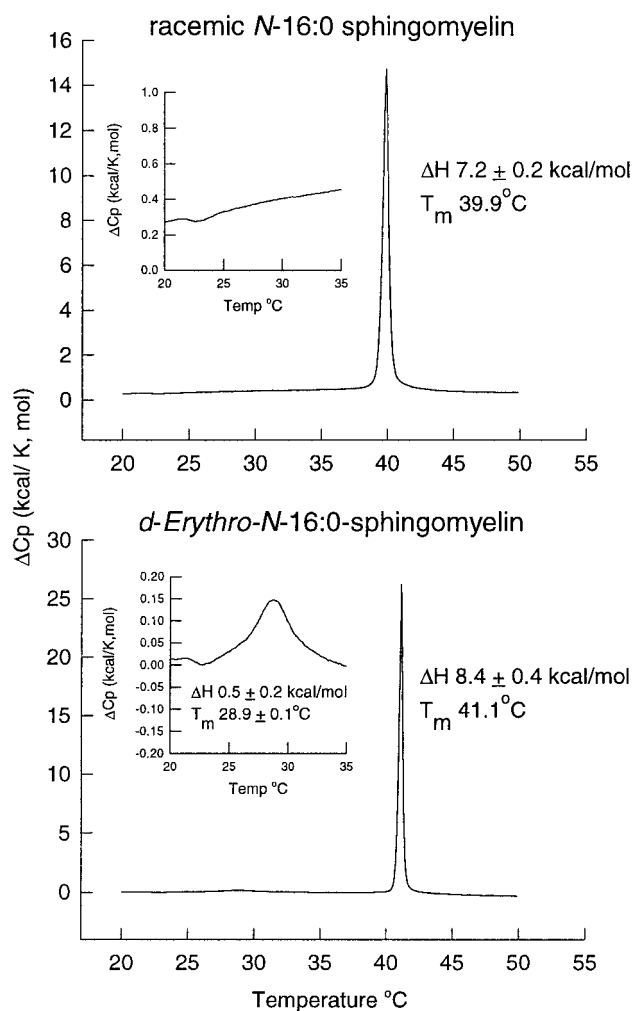


FIGURE 4 Heat capacity versus temperature curves for purified racemic *N*-16:0-SM and *d*-erythro-*N*-16:0-SM suspensions.

### Steady-state anisotropy for sphingomyelins in unilamellar vesicles

To study the steady-state anisotropy of the bilayer core and interface regions, respectively, DPH and TMA-DPH were used as reporter molecules (Prendergast et al., 1981). With TMA-DPH as a probe, the anisotropy value was observed to be significantly higher for *d-erythro-N-16:0-SM* than for the corresponding racemic sphingomyelin, both with and without cholesterol (Table 3). This finding suggests a tighter packing at the interface of the *d-erythro-N-16:0-SM* vesicles, compared with the racemic counterpart. The packing of the acyl chains in the bilayer seemed to be unaffected by the stereochemistry, because there were no apparent differences in the steady-state anisotropy values when DPH was used as a probe.

### Sphingomyelin hydrolysis in monolayers by bacterial sphingomyelinase

The degradation of sphingomyelin in monolayers by sphingomyelinase in the subphase can be followed as a time-dependent reduction in the monolayer area, because the reaction product (i.e., ceramide) has a smaller molecular area requirement than sphingomyelin (Yedgar et al., 1982; Jungner et al., 1997). The degradation of racemic sphingomyelin and that of *d-erythro-N-16:0-SM* by 67 mU/ml sphingomyelinase in the subphase are compared in Fig. 5 A. The time needed to reach half-maximum degradation ( $T_{50\%}$ ) was  $\sim 10$  times longer for *d-erythro-N-16:0-SM* than it was for the corresponding racemic sphingomyelin (1.8 and 18 min, respectively). The rate of *d-erythro-N-16:0-SM* degradation was so slow that a 10-fold higher sphingomyelinase concentration had to be used to obtain a reasonable degradation time (cf. Jungner et al., 1997). The degradation of the more fluid *N-18:1-SMs* was faster and was accomplished at a lower sphingomyelinase activity (6.7 mU/ml). Still, the racemic *N-18:1-SMs* degraded faster than the *d-erythro-N-18:1-SM* (Fig. 5 B).

**TABLE 3** Steady-state anisotropy of DPH and TMA-DPH in pure sphingomyelin vesicles\*

Lipid composition	DPH	TMA-DPH
Racemic <i>N-16:0-SM</i>	$0.348 \pm 0.003$	$0.348 \pm 0.003$
Racemic <i>N-16:0-SM</i> + cholesterol	$0.323 \pm 0.003$	$0.343 \pm 0.003$
<i>d-Erythro-N-16:0-SM</i>	$0.343 \pm 0.003$	$0.370 \pm 0.005$
<i>d-Erythro-N-16:0-SM</i> + cholesterol	$0.320 \pm 0.001$	$0.358 \pm 0.002$
Racemic <i>N-18:1-SM</i>	$0.175 \pm 0.001$	$0.258 \pm 0.002$
Racemic <i>N-18:1-SM</i> + cholesterol	$0.253 \pm 0.007$	$0.293 \pm 0.008$
<i>d-Erythro-N-18:1-SM</i>	$0.168 \pm 0.008$	$0.260 \pm 0.001$
<i>d-Erythro-N-18:1-SM</i> + cholesterol	$0.263 \pm 0.008$	$0.295 \pm 0.005$

\*Unilamellar vesicles were prepared at 55°C by extrusion through 400-nm polycarbonate filters from pure sphingomyelins or from a mixture of 30 mol% cholesterol and 70 mol% sphingomyelin. Anisotropy measurements were carried out at 20°C with DPH or TMA-DPH as a fluorescent probe. Values are given as the average value  $\pm$  range from two different batches of vesicles.

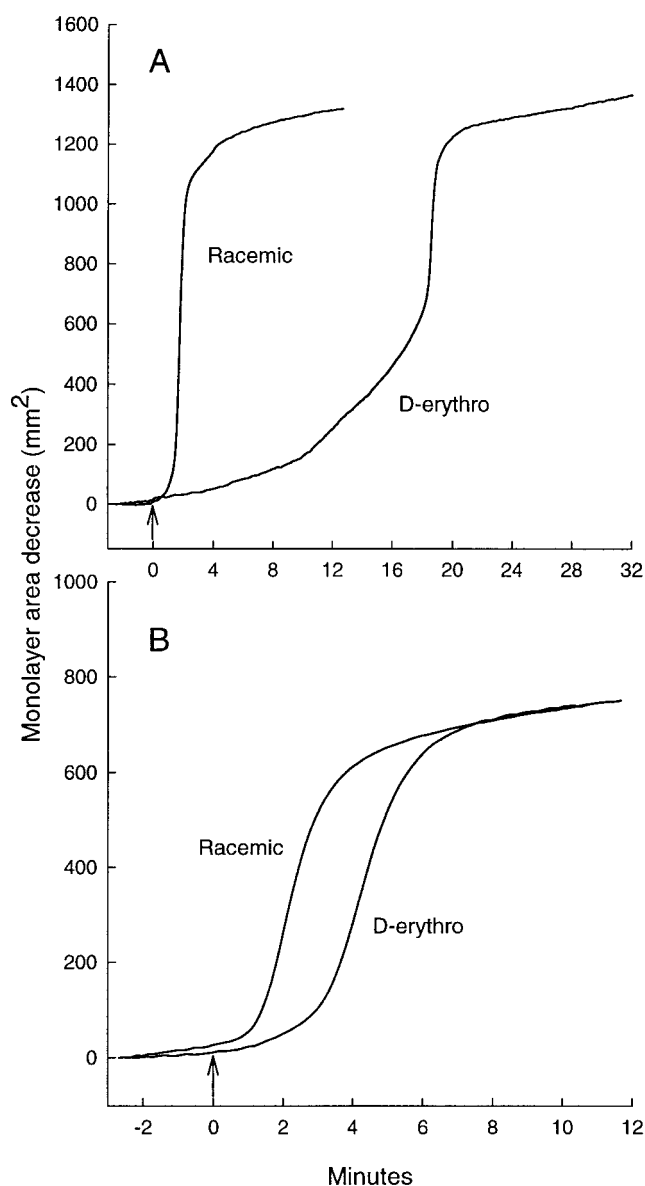


**FIGURE 5** Hydrolysis of monolayer sphingomyelin by bacterial sphingomyelinase. Pure sphingomyelin monolayers were prepared at the air/buffer interface and were kept at a constant surface pressure of 20 mN/m. Sphingomyelinase was added to the stirred subphase to a final activity of 6.7 mU/ml for *N-18:1-SMs* and 67 mU/ml for *N-16:0-SMs*. Degradation of sphingomyelin by the enzyme led to a monolayer area decrease that is plotted as a time function.

### DISCUSSION

This work was conducted to compare the biophysical properties of the naturally occurring *d-erythro* isomer of sphingomyelin with acyl-chain-matched racemic (*d-erythro/l-threo*) sphingomyelin. The results of this study show that there are differences in the properties of pure *d-erythro*-sphingomyelins compared with racemic sphingomyelins, especially for the saturated *N-16:0-SM*. In monolayer membranes containing only sphingomyelin, the force-area measurements indicated that the pure *d-erythro-N-16:0-SM*

molecules had a slightly smaller mean molecular area requirement than the racemic counterpart, when present in the liquid-expanded state (i.e., below the transition pressure). This difference was overcome by compression, because isotherms of *N*-16:0-SMs in their liquid-condensed state were indistinguishable. The liquid-expanded to liquid-condensed phase transition was also sharper and occurred at a lower surface pressure in *d-erythro-N*-16:0-SM monolayers as compared with racemic *N*-16:0-SM monolayers, again suggesting that *d-erythro-N*-16:0-SMs packed more efficiently in the monolayer membrane. The tighter packing and/or the stereochemical orientation of the 3-OH function in the sphingomyelins appeared to affect the degree of cooperativity in the transition (Israelachvili, 1994). With monounsaturated sphingomyelins, no difference was seen in force-area isotherms between the racemic and *d-erythro* species, suggesting that the higher degree of disorder in the acyl chain region (resulting in increased spacing between molecules) diminished the possible effects of racemization in the interfacial region.

The formation of laterally condensed domains in monolayer membranes can be documented with monolayer fluorescence microscopy and a suitable fluorescence probe (von Tscharner and McConnell, 1981; Slotte and Mattjus, 1995). The mixing of cholesterol into dipalmitoyl phosphatidylcholine or racemic *N*-16:0-SM monolayers has been shown to result in the formation of cholesterol-rich condensed domains, the number of which increases with increasing cholesterol concentration (Slotte, 1995). Here we show that in *N*-16:0-SM monolayers, cholesterol formed larger condensed domains with *d-erythro-N*-16:0-SM as compared with racemic *N*-16:0-SM. This finding indicates that the dipole-induced and/or electrostatic repulsion of cholesterol-enriched condensed domains (Subramaniam and McConnell, 1987; Keller et al., 1987; Seul and Sammon, 1990) was easier to overcome when pure *d-erythro*-sphingomyelin was the matrix, as compared with the racemic system. However, although these differences were seen in compressed and reexpanded monolayers, the domains seen may not completely represent the equilibrium state, but may also be influenced by dynamic differences.

Because strong intermolecular interactions between cholesterol and a phospholipid affect the energy needed for cholesterol to desorb from the membrane, desorption rates can be used to estimate relative strengths of interactions in model and biological membranes (Phillips et al., 1987; Bittman, 1988; Ohvo and Slotte, 1996). Cholesterol desorption from monolayers to CyD acceptors is known to be much slower from sphingomyelin monolayers than from acyl-chain-matched phosphatidylcholine monolayers (Ramstedt and Slotte, 1999). In this study we observed that cholesterol desorption to CyD was significantly lower from mixed monolayers containing *d-erythro-N*-16:0-SM than it was from monolayers with racemic *N*-16:0-SM (Table 2). This finding clearly indicates a stronger interaction between cholesterol and *d-erythro-N*-16:0-SM than between cholesterol and the racemic counterpart. This effect on cholesterol

desorption was most likely due to effects of *d-erythro-N*-16:0-SM on monolayer packing properties (denser packing), because racemization did not affect cholesterol desorption rates from monounsaturated sphingomyelin monolayers, in which the packing also was not affected.

The tighter lateral packing of *d-erythro-N*-16:0-SM was also seen in bilayer membranes. The onset of the main phase transition for *d-erythro-N*-16:0-SM took place at a higher temperature (41.1°C) than that for the racemic *N*-16:0-SM (39.9°C) when studied by DSC. The higher transition temperature, as well as the higher molar enthalpy for *d-erythro-N*-16:0-SM melting, is compatible with closer packing and hence more cohesive attractive interactions among the *d-erythro-N*-16:0-SM in the vesicles. The gel-to-liquid transition temperature observed in this study agrees well with the  $T_m$  reported for a comparable, fully synthetic *d-erythro-N*-16:0-SM that was examined by Bar and co-workers (1997). The molar enthalpy we report is slightly higher than that reported by Bar et al. (1997) ( $8.4 \pm 0.4$  versus  $6.8 \pm 0.2$  kcal/mol). This small difference is probably due to a slight difference in phosphate calibration during chemical analysis of the sphingomyelins. The finding that racemic *N*-16:0-SM showed both a lower  $T_m$  and a lower molar enthalpy ( $7.2 \pm 0.2$  kcal/mol) compared to *d-erythro-N*-16:0-SM is significant, because the results were obtained in the same laboratory, using identical purification and chemical assay procedures. Our thermograms with *d-erythro-N*-16:0-SM also displayed a reproducible pretransition at 28.9°C, which also has been reported by Bar and co-workers (1997). This apparent  $L_{\beta'}$ -to- $P_{\beta'}$  transition was not seen in vesicles prepared from racemic *N*-16:0-SM, probably because of packing constraints resulting from the racemization of the 3-OH function.

Steady-state anisotropy measurements of DPH and TMA-DPH in racemic or *d-erythro* sphingomyelin unilamellar vesicles were also performed in this study. DPH is known to partition equally between condensed and liquid domains and is known to localize to the hydrocarbon core of the membrane bilayer (Shinitzky and Barenholz, 1978), whereas TMA-DPH (being positively charged) is found in the interfacial region of the membrane (Prendergast et al., 1981). Our findings show that the anisotropy (and hence packing density) was higher in the interfacial region of *d-erythro-N*-16:0-SM compared with racemic *N*-16:0-SM. These results agree nicely with our monolayer and DSC results, implying that *d-erythro-N*-16:0-SM packing is different from racemic *N*-16:0-SM packing. The anisotropy of the bilayer core was not affected, however, by racemization of the 3-OH function. No difference in anisotropy (for either DPH or TMA-DPH) was seen in *d-erythro* or racemic monounsaturated sphingomyelin vesicles. The effects of cholesterol on the anisotropies of DPH and TMA-DPH were expected; i.e., it decreased the core and interface anisotropy in saturated sphingomyelin vesicles and increased it in monounsaturated sphingomyelin vesicles (see, e.g., McMullen and McElhaney, 1996).



Finally, the hydrolysis of sphingomyelin in pure monolayers by bacterial sphingomyelinase was seen to be markedly affected by the stereochemistry of the sphingomyelin substrate molecules. Sphingomyelin hydrolysis has previously been shown to be affected by the phase state of the molecules in the membrane, for both monolayers and bilayers (Jungner et al., 1997; Cohen and Barenholz, 1978). We now observed that the time needed for 50% completion of the hydrolytic reaction was dramatically longer with the naturally occurring *d*-erythro isomers than it was with the corresponding racemic sphingomyelins. This difference was especially true for *d*-erythro-*N*-16:0-SM, because a much higher enzyme activity (10-fold) was needed to accomplish degradation compared with, e.g., *N*-18:1-SMs. The slow onset of hydrolysis in *d*-erythro-*N*-16:0-SM monolayers can be explained in part by the tighter lateral packing seen in this monolayer. A tighter and more optimal packing density also leads to fewer packing defects in the monolayer, sites where the enzyme probably interacts (initially) with the monolayer. However, because the degradation of *d*-erythro-*N*-18:1-SM was significantly slower than the degradation of the racemic counterpart, it is likely that effects other than packing density (which is almost similar for racemic and *d*-erythro-*N*-18:1-SM) also affected the enzyme-catalyzed degradation rates. It is not clear from this study what these effects could be.

In conclusion, this study has demonstrated that racemic sphingomyelins differ significantly from their naturally occurring *d*-erythro counterparts, and it is therefore strongly suggested that future biophysical studies of sphingomyelins should utilize the *d*-erythro analogs as models for the naturally occurring sphingomyelins.

We thank Prof. Jorma Mattinen for performing the NMR analysis and Ms. Anna Lind for technical assistance.

This research was supported by generous grants from the Academy of Finland, the Sigrid Juselius Foundation, the Oscar Öflund Foundation, and the Åbo Akademi University.

## REFERENCES

- Bar, L. K., Y. Barenholz, and T. E. Thompson. 1997. Effect of sphingomyelin composition on the phase structure of phosphatidylcholine-sphingomyelin bilayers. *Biochemistry*. 36:2507–2516.
- Barenholz, Y., and T. E. Thompson. 1980. Sphingomyelins in bilayers and biological membranes. *Biochim. Biophys. Acta*. 604:129–158.
- Bittman, R. 1988. Sterol exchange between mycoplasma membranes and vesicles. In *Biology of Cholesterol*. P. L. Yeagle, editor. CRC Press, Boca Raton, FL. 173–195.
- Bittman, R., C. R. Kasireddy, P. Mattjus, and J. P. Slotte. 1994. Interaction of cholesterol with sphingomyelin in monolayers and vesicles. *Biochemistry*. 33:11776–11781.
- Boggs, J. M. 1987. Lipid intermolecular hydrogen bonding: influence on structural organization and membrane function. *Biochim. Biophys. Acta*. 906:353–404.
- Brown, D. A., and J. K. Rose. 1992. Sorting of GPI-anchored proteins to glycolipid-enriched membrane subdomains during transport to the apical cell surface. *Cell*. 68:533–544.
- Brown, R. E. 1998. Sphingolipid organization in biomembranes: what physical studies of model membranes reveal. *J. Cell Sci.* 111:1–9.
- Bruzik, K. S. 1987. A calorimetric study of the thermotropic behavior of pure sphingomyelin diastereomers. *Biochemistry*. 26:5364–5368.
- Bruzik, K. S. 1988. Conformation of the polar headgroup of sphingomyelin and its analogues. *Biochim. Biophys. Acta*. 939:315–326.
- Cohen, R., and Y. Barenholz. 1978. Correlation between the thermotropic behavior of sphingomyelin liposomes and sphingomyelin hydrolysis by sphingomyelinase of *Staphylococcus aureus*. *Biochim. Biophys. Acta*. 509:181–187.
- Cohen, R., Y. Barenholz, S. Gatt, and A. Dagan. 1984. Preparation and characterization of well defined *D*-erythro sphingomyelins. *Chem. Phys. Lipids*. 35:371–384.
- Gaver, R. C., and C. C. Sweeley. 1965. Methods for methanolysis of sphingolipids and direct determination of long-chain bases by gas chromatography. *J. Am. Oil Chem. Soc.* 42:294–298.
- Grönberg, L., Z. S. Ruan, R. Bittman, and J. P. Slotte. 1991. Interaction of cholesterol with synthetic sphingomyelin derivatives in mixed monolayers. *Biochemistry*. 30:10746–10754.
- Harder, T., and K. Simons. 1997. Caveolae, DIGs, and the dynamics of sphingolipid-cholesterol microdomains. *Curr. Opin. Cell Biol.* 9:534–542.
- Hope, M. J., M. B. Bally, G. Webb, and P. R. Cullis. 1985. Production of large unilamellar vesicles by a rapid extrusion procedure. Characterization of size distribution, trapped volume and ability to maintain a membrane potential. *Biochim. Biophys. Acta*. 812:55–65.
- Israelachvili, J. 1994. Self-assembly in two dimensions: surface micelles and domain formation in monolayers. *Langmuir*. 10:3774–3781.
- Jungner, M., H. Ohvo, and J. P. Slotte. 1997. Interfacial regulation of bacterial sphingomyelinase activity. *Biochim. Biophys. Acta*. 1344:230–240.
- Kaluzny, M. A., L. A. Duncan, M. V. Merritt, and D. E. Epps. 1985. Rapid separation of lipid classes in high yield and purity using bonded phase columns. *J. Lipid Res.* 26:135–140.
- Kan, C.-C., Z.-s. Ruan, and R. Bittman. 1991. Interaction of cholesterol with sphingomyelin in bilayer membranes: evidence that the hydroxy group of sphingomyelin does not modulate the rate of cholesterol exchange between vesicles. *Biochemistry*. 30:7759–7766.
- Keller, D. J., J. P. Korb, and H. M. McConnell. 1987. Theory of shape transition in two-dimensional phospholipid domains. *J. Phys. Chem.* 91:6417–6422.
- Lakowicz, J. R. 1983. *Principles of Fluorescence Spectroscopy*. Plenum Press, New York.
- Lange, Y., and B. V. Ramos. 1983. Analysis of the distribution of cholesterol in the intact cell. *J. Biol. Chem.* 258:15130–15134.
- Lange, Y., M. H. Swaisgood, B. V. Ramos, and T. L. Steck. 1989. Plasma membranes contain half the phospholipid and 90% of the cholesterol and sphingomyelin in cultured human fibroblasts. *J. Biol. Chem.* 264:3786–3793.
- Maulik, P. R., and G. G. Shipley. 1996. *N*-Palmitoyl sphingomyelin bilayers: structure and interactions with cholesterol and dipalmitoylphosphatidylcholine. *Biochemistry*. 35:8025–8034.
- Maulik, P. R., P. K. Sripada, and G. G. Shipley. 1991. Structure and thermotropic properties of hydrated *N*-stearoyl sphingomyelin bilayer membranes. *Biochim. Biophys. Acta*. 1062:211–219.
- McMullen, T. P. W., and R. N. McElhaney. 1996. Physical studies of cholesterol-phospholipid interactions. *Curr. Opin. Colloid Interface Sci.* 1:83–90.
- Moesby, L., J. Corver, R. K. Erukulla, R. Bittman, and J. Wilschut. 1995. Sphingolipids activate membrane fusion of Semliki Forest virus in a stereospecific manner. *Biochemistry*. 34:10319–10324.
- Morrison, W. R., and J. D. Hay. 1970. Polar lipids in bovine milk. II. Long-chain bases, normal and 2-hydroxy fatty acids, and isomeric cis and trans monoenoic fatty acids in the sphingolipids. *Biochim. Biophys. Acta*. 202:460–467.
- Nag, K., and K. M. Keough. 1993. Epifluorescence microscopic studies of monolayers containing mixtures of dioleoyl- and dipalmitoylphosphatidylcholines. *Biophys. J.* 65:1019–1026.
- Ohvo, H., C. Olsio, and J. P. Slotte. 1997. Effects of sphingomyelin and phosphatidylcholine degradation on cyclodextrin-mediated cholesterol efflux in cultured fibroblasts. *Biochim. Biophys. Acta*. 1349:131–141.



- Ohvo, H., and J. P. Slotte. 1996. Cyclodextrin-mediated removal of sterols from monolayers: effects of sterol structure and phospholipids on desorption rate. *Biochemistry*. 35:8018–8024.
- Phillips, M. C., W. J. Johnson, and G. H. Rothblat. 1987. Mechanisms and consequences of cellular cholesterol exchange and transfer. *Biochim. Biophys. Acta*. 906:223–276.
- Pörn, M. I., M. P. Ares, and J. P. Slotte. 1993. Degradation of plasma membrane phosphatidylcholine appears not to affect the cellular cholesterol distribution. *J. Lipid Res.* 34:1385–1392.
- Prendergast, F. G., R. P. Haugland, and P. J. Callahan. 1981. 1-[4-(Trimethylamino)phenyl]-6-phenylhexa-1,3,5-triene: synthesis, fluorescence properties, and use as a fluorescence probe in lipid bilayers. *Biochemistry*. 20:7333–7338.
- Ramstedt, B., and J. P. Slotte. 1999. Interaction of cholesterol with sphingomyelins and acyl-chain-matched phosphatidylcholines—a comparative study of the effect of the chain length. *Biophys. J.* 76:908–915.
- Schroeder, F., A. A. Frolov, E. J. Murphy, B. P. Atshaves, J. R. Jefferson, L. Pu, G. W. Wood, W. B. Foxworth, and A. B. Kier. 1996. Recent advances in membrane cholesterol domain dynamics and intracellular cholesterol trafficking. *Proc. Soc. Exp. Biol. Med.* 213:150–177.
- Seul, M., and M. J. Sammon. 1990. Competing interactions and domain-shape instabilities in a monomolecular film at the air/water interface. *Phys. Rev. Lett.* 64:1903–1906.
- Shinitzky, M., and Y. Barenholz. 1978. Fluidity parameters of lipid regions determined by fluorescence polarization. *Biochim. Biophys. Acta*. 515:367–394.
- Simons, K., and E. Ikonen. 1997. Functional rafts in cell membranes. *Nature*. 387:569–572.
- Skipski, V. P., R. F. Peterson, and M. Barclay. 1964. Quantitative analysis of phospholipids by thin-layer chromatography. *Biochem. J.* 90:374–378.
- Slotte, J. P. 1995. Lateral domain formation in mixed monolayers containing cholesterol and dipalmitoylphosphatidylcholine or *N*-palmitoylsphingomyelin. *Biochim. Biophys. Acta*. 1235:419–427.
- Slotte, J. P., and P. Mattjus. 1995. Visualization of lateral phases in cholesterol and phosphatidylcholine monolayers at the air/water interface—a comparative study with two different reporter molecules. *Biochim. Biophys. Acta*. 1254:22–29.
- Smaby, J. M., V. S. Kulkarni, M. Momsen, and R. E. Brown. 1996. The interfacial elastic packing interactions of galactosylceramides, sphingomyelins, and phosphatidylcholines. *Biophys. J.* 70:868–877.
- Sripada, P. K., P. R. Maulik, J. A. Hamilton, and G. G. Shipley. 1987. Partial synthesis and properties of a series of *N*-acyl sphingomyelins. *J. Lipid Res.* 28:710–718.
- Subramaniam, S., and H. M. McConnell. 1987. Critical mixing in monolayer mixtures of phospholipid and cholesterol. *J. Phys. Chem.* 91:1715–1718.
- Verger, R., and G. H. de Haas. 1973. Enzyme reactions in a membrane model. I. A new technique to study enzyme reactions in monolayers. *Chem. Phys. Lipids*. 10:127–136.
- von Tschärner, V., and H. M. McConnell. 1981. An alternative view of phospholipid phase behavior at the air-water interface. *Biophys. J.* 36:409–419.
- Wilson, E., E. Wang, R. E. Mullins, D. J. Uhlinger, D. C. Liotta, J. D. Lambeth, and A. H. Merrill, Jr. 1988. Modulation of the free sphingosine levels in human neutrophils by phorbol esters and other factors. *J. Biol. Chem.* 263:9304–9309.
- Yedgar, S., R. Cohen, S. Gatt, and Y. Barenholz. 1982. Hydrolysis of monomolecular layers of synthetic sphingomyelins by sphingomyelinase of *Staphylococcus aureus*. *Biochem. J.* 201:597–603.